ELSEVIER

Polymer 42 (2001) 9513–9522

polymer

www.elsevier.com/locate/polymer

Effect of melt processing conditions on the extent of exfoliation in organoclay-based nanocomposites

H.R. Dennis[a], D.L. Hunter[a,*], D. Chang[b], S. Kim[b], J.L. White[b], J.W. Cho[c], D.R. Paul[c,*]

[a]*Southern Clay Products, 1212 Church St., Gonzales, TX 78629, USA*
[b]*Institute of Polymer Engineering, The University of Akron, Akron, OH 44235, USA*
[c]*Department of Chemical Engineering, Texas Material Institute, The University of Texas at Austin, Austin, TX 78712, USA*

Received 11 April 2001; received in revised form 22 June 2001; accepted 25 June 2001

Abstract

Polymer layered silicate nanocomposites have been studied for nearly 50 years, but few references deal with the importance of how the organoclay was processed into the plastic of choice. Many articles focus on the importance of the chemistry used to modify the surface of the clay, usually montmorillonite, without including the role of processing. This paper demonstrates the importance of both the chemistry of the clay surface and how the clay was melt processed into the thermoplastic. Two different clay treatments were added to polyamide 6 using four different types of extruders with multiple screw designs. The mixtures of organoclay and polyamide 6 were characterized by X-ray diffraction, transmission electron microscopy, and mechanical property tests. The degree of dispersion is interpreted in terms of the residence time distribution in the extruder and the intensity of shear. A model for organoclay delamination in a polymer melt is proposed that envisions the role of both shear and time.

Keywords: Polymer; Nanocomposites; Organoclay

1. Introduction

Polymer layered silicate nanocomposites were reported in the patent literature as early as 1950 [1]. Polyamide nanocomposites were reported as early as 1976 [2]. However, it was not until Toyota researchers [3–6] began a detailed examination of polymer layered silicate clay mineral composites that nanocomposites became more widely studied in academic, government and industrial laboratories. The early Toyota work is based on formation of nanocomposites in situ during polymerization of caprolactam. Nanocomposites can be made in this way from both thermoplastic and thermoset resins. However, there is ample evidence that nanocomposites can also be formed by melt processing. While it might be anticipated that melt processing conditions would have an important influence on the nature of the nanocomposite formed, until recently the literature contained no summary conclusions about the optimum process conditions needed [7]. There are many reasons why melt processing may be the more preferred method for producing nanocomposites for commercial use. This paper describes a collaboration aimed at examination of the effects of processing conditions on the formation of nanocomposites from a thermoplastic and an organoclay.

The nanocomposites of interest here are made from polymers and layered silicate clay minerals. The organoclay is based on montmorillonite (MMT) which has high surface area, about 750 m^2/g; a large aspect ratio, greater than 50; a platelet thickness of 10 Å. While nanocomposites can be made from organoclays in a number of ways [8], this work deals with melt blending the clay into the polymer. Nanocomposites formed by melt blending have been described previously [7–16]; however, these studies have not addressed the issues of how the resulting structure is affected by the design of the mixing device. This paper describes an extensive study on how the extruder type and screw design affect the degree of dispersion of MMT platelets in a polyamide matrix. The inorganic MMT surface is modified by organic treatments to make the platelet more compatible with the organic polymer. It is well documented that the choice of the organic treatment influences the degree of dispersion of the MMT in the polymer matrix [10–13,17]. It is shown here that the degree of delamination of the MMT platelets and their dispersion in the matrix polymer are also significantly influenced by the details of the melt blending process.

Unlike the more common clay minerals used as fillers for

* Corresponding authors. Tel.: +1-512-471-5238; fax: +1-512-471-0542.
E-mail address: drp@che.utexas.edu (D.R. Paul).

0032-3861/01/$ - see front matter
PII: S0032-3861(01)00473-6

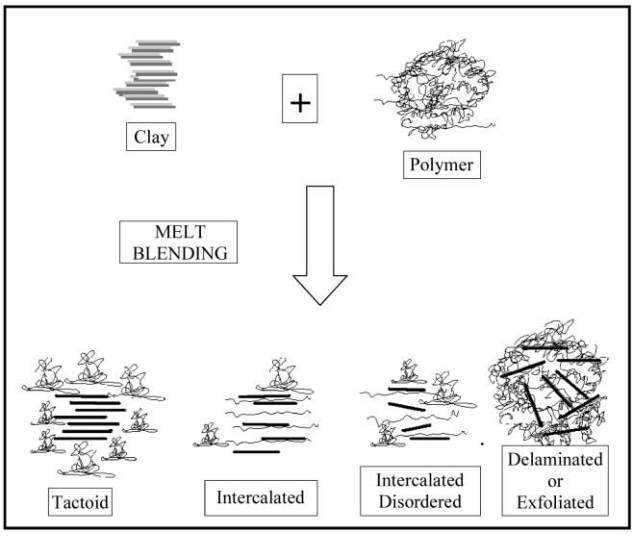

Fig. 1. Schematic illustration of terminology used to describe nanocomposites formed from organoclays.

plastics, such as talc and mica, MMT can be delaminated and dispersed into individual layers of only 10 Å thickness. Unseparated MMT layers, after introduction into the polymer, are often referred to as tactoids [17,18]. The term intercalation describes the case where a small amount of polymer moves into the gallery spacing between the clay platelets, but causes less than 20–30 Å separation between the platelets. Exfoliation or delamination occurs when polymer further separates the clay platelets, e.g. by 80–100 Å or more. A well-delaminated and dispersed nanocomposite consists of delaminated platelets distributed homogeneously in the polymer. These terms are shown schematically in Fig. 1.

The organoclays used to form the nanocomposites here are products of Southern Clay Products, marketed under the trademark Cloisite®, that are supplied as particles nominally 8 μm in size. A key to the benefits of MMT in nanocomposites, but the challenge in processing to make the nanocomposite, is that there are, perhaps, a million or more platelets in each 8 μm particle. For most applications, it is generally believed that maximum benefits are achieved when the platelets are well dispersed.

Numerous benefits of nanocomposites formed from a variety of matrix polymers have been described. The property improvements can generally be divided into the following areas: mechanical properties, heat resistance, dimensional stability, barrier and flame retardation. The potential property improvements usually depend on the degree of delamination and dispersion, which, as shown here, depends on a combination of the proper chemical treatment and optimized processing.

2. Materials and characterization

Polyamide 6, Capron B135WP from Honeywell, was melt blended with two organoclays, Cloisite 15A (15A) and Cloisite 30B (30B). Capron B135WP has a melt flow index of 12 and a number average molecular weight of 30,000 g/mol. The MMT for the Cloisites is refined from a Wyoming bentonite and has a cation exchange capacity of 92 meq/100 g clay. Cloisite 15A is treated with 125 meq/100 g clay of Arquad 2HT from Akzo Nobel, dimethyldihydrogenatedtallow quaternary ammonium chloride. Cloisite 30B is exchanged with 90 meq/100 g clay of Ethoquad T12, methyl bis-2-hydroxyethyltallow quaternary ammonium chloride.

Several combinations of extruders and screw configurations were employed for melt blending the organoclays in this polyamide 6 matrix. A 5 wt% loading of the organoclay, a powder with a mean particle size of 8 μm, and the polyamide pellets were premixed in a tumbler. Because the equivalent weight of the quaternary ammonium salts and the actual loading levels are different, the mineral content of the final nanocomposite is different. The mineral contents of the nanocomposite generated here from 30B and 15A are 3.7 and 3.1%, respectively.

The degree of delamination and dispersion of the compounded nanocomposite was monitored by wide-angle X-ray or XRD (Sintag XDS 2000) in the reflectance mode, and transmission electron microscopy or TEM (Phillips/EM 301 at 80 keV). XRD results were analyzed by considering changes in the basal spacing (d-spacing) and the area under the peak. The level of dispersion as judged by TEM was quantified by counting the number of platelets or intercalates seen in twelve 6.25 cm^2 cutouts from a sheet of paper laid over a photomicrograph printed at 130,500× magnification and averaging them to give a number representing the delamination and dispersion for that TEM photomicrograph. The higher the number is the better the delamination and dispersion is. The average number of platelets/intercalates seen in this specified area will be referred to as the 'TEM Dispersion'. Physical properties were determined following ASTM D638 and D256A methods.

3. Extruder types, screw configurations and residence time distributions

Experimental studies of blending the MMT into polyamide 6 were carried out in four extruders using a variety of screw designs shown in Figs. 2–4. This is not an exhaustive study of mixer types, but is meant to include enough variety to demonstrate the importance of the process for making nanocomposites. The extruders were a Killion 25.4 mm single screw extruder outfitted with a high intensity mixing head, a Japan Steel Works 30 mm modular self-wiping co-rotating twin screw extruder [19], a Leistritz 34 mm modular intermeshing, counter-rotating twin screw extruder [19,20], and a Leistritz 34 mm modular non-intermeshing, counter-rotating twin screw extruder [21]. For each twin screw extruder type, the shear intensity of mixing was

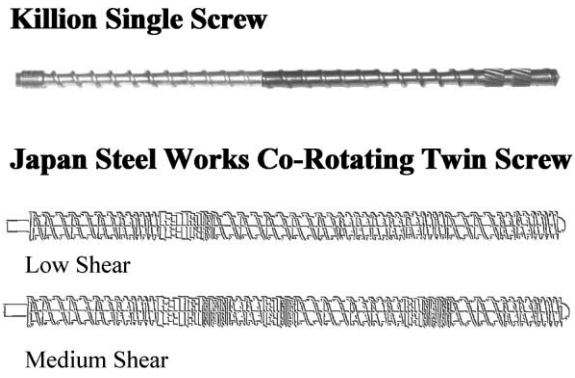

Fig. 2. Screw configurations used in the single screw and co-rotating twin screw extruders.

changed by changing the screw configuration. The descriptors low, medium and high shear intensity screw configurations used below are a qualitative indication of the intensity of mixing and are only meaningful within the extruder type.

Two screw configurations were evaluated for the JSW co-rotating extruder. The co-rotating screw configurations used in this study differ in the number of kneading disc blocks in the screw. The low shear intensity screw had one kneading block early in the screw to melt the resin and thereby maximize the time the organoclay mixes with the molten resin. The medium shear intensity configuration incorporated three kneading block sections. Kneading disc block sections can be made up of different width paddles, the wider the paddle the more elongational shear and dispersive mixing. Narrow width discs favor distributive mixing and impose less shear intensity. The discs in the kneading block can be fabricated at different staggering angles to facilitate movement of the resin forward, reverse or not at all. This allows the residence time a given element of polymer stays within the kneading block, and thus the screw, to be varied by changing the elements. Within a kneading block section, a forward pumping kneading section typically precedes a reverse or neutral kneading section. The inclusion of a reverse or neutral kneading element in the kneading block section causes an element of polymer to spend more time in the kneading block and increases the shear intensity of the screw configuration.

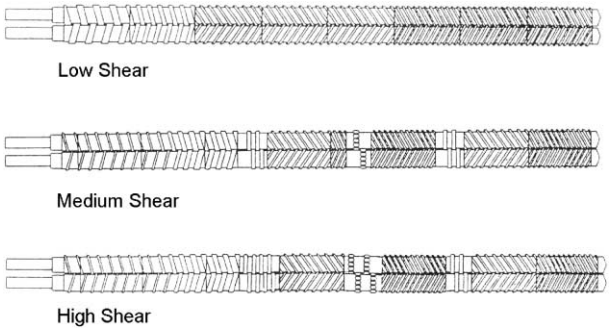

Fig. 3. Screw configurations used in the counter-rotating, intermeshing twin screw extruder.

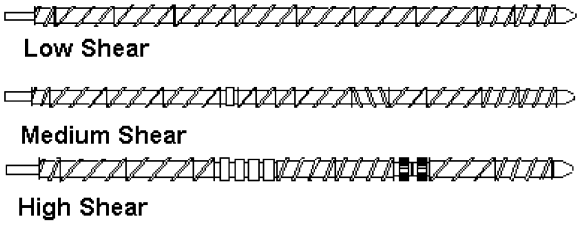

Fig. 4. Screw configurations used in the counter-rotating, non-intermeshing twin screw extruder.

Leistritz counter-rotating extruders do not use kneading blocks. There are both intermeshing and non-intermeshing (tangential) counter-rotating extruder types that are included in the study reported in this paper. The intermeshing extruder will traditionally impart more shear intensity than the non-intermeshing extruder will. The non-intermeshing extruder is generally regarded as a low shear extruder that favors distributive mixing. For the counter-rotating intermeshing extruder, the conveying elements vary from closed (higher shear) to open flighted (lower shear). Three screw configurations were used for the Leistritz counter-rotating extruder in both the intermeshing and non-intermeshing mode. For the intermeshing mode, the low shear intensity configuration is roughly a closed flighted positive displacement pump; the medium shear intensity configuration is a closed flighted pump to which two sets of two shearing elements each and a turbine distributive mixer (slit stowing element) have been added; and the high shear intensity configuration is a close flighted pump to which two sets of four shearing elements and two shearing elements and a set of two turbine distributive mixer elements have been added. The shearing elements not only increase the extensional flow, but also increase the residence time as they create an additional barrier for the polymer to move through. For the non-intermeshing mode, the low shear intensity configuration is a simple, open flighted distributive mixer; the medium shear intensity configuration has a shearing element and a reverse element added; and the high shear intensity configuration is a distributive mixer with a set of four shearing elements and a set of two turbines.

For the twin screw extruders, the following were held constant: feed rate of 5 kg/h, temperature of 240°C, screw speed of 200 rpm and a nominal 30 mm screw. For the single screw extruder, a lower feed rate and screw speed (40 rpm) were used. These conditions gave the residence time distribution curves shown in Figs. 5–7 measured by spiking a pulse of 1–2 mm aluminum pellets to the feed hopper at time $t = 0$ as described previously [19]. The extruder can be thought of as a tubular mixer having a certain mean residence time and degree of backmixing, which can be quantified by calculating the following moments of the residence time distribution curves.

$$M_1 = \int_0^\infty tC(t)\,\mathrm{d}t / \int_0^\infty C(t)\,\mathrm{d}t \tag{1}$$

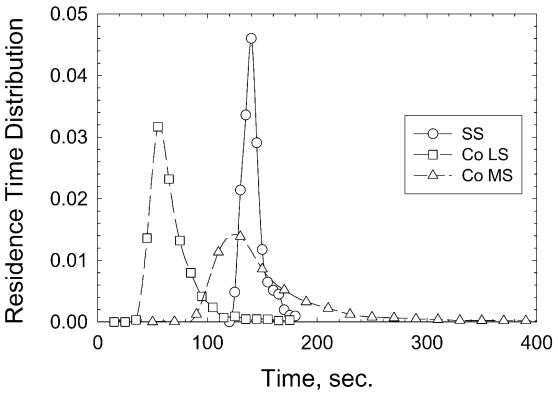

Fig. 5. Residence time distribution curves for the single screw extruder (SS) and the co-rotating twin screw extruder outfitted with low (Co LS) and medium (Co MS) shear screw configurations.

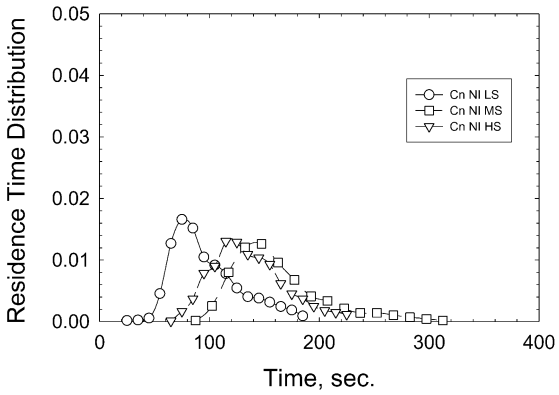

Fig. 7. Residence time distribution curves for the counter-rotating, intermeshing twin screw extruder outfitted with the low (Cn I LS), medium (Cn I MS), and high (CN I HS) shear screw configurations.

$$M_2 = \int_0^\infty t^2 C(t)\,\mathrm{d}t \Big/ \int_0^\infty C(t)\,\mathrm{d}t \tag{2}$$

where $C(t)$ is the concentration of aluminum tracer in the extrudate at time t. Since the extrudate was sampled at fixed time intervals Δt, the integrals can be conveniently converted to summations [19] and the calculations executed by a spreadsheet program. The first moment is simply the mean residence time $\bar{t}$ which is related to the volumetric flow rate (Q), total volume between the screw and barrel, (V_{total}), and the fill factor (Φ) as follows:

$$\bar{t} = M_1 = \Phi V_{\text{total}}/Q \tag{3}$$

The variance of the distribution about the mean is given by

$$\sigma_t^2 = M_2 - \bar{t}^2 \tag{4}$$

Since the variance σ_t^2 scales by $\bar{t}^2$, it is more meaningful to define the following normalized and dimensionless variance

$$\sigma^2 = \sigma_t^2/\bar{t}^2 \tag{5}$$

If polymer melt flowed through the extruder as a plug with no backmixing, σ^2 would be zero. The normalized variance σ^2 is a quantitative measure of the extent of backmixing in the extruder. Values of $\bar{t}$ and σ^2 calculated from the data in Figs. 5–7 are listed in Table 1.

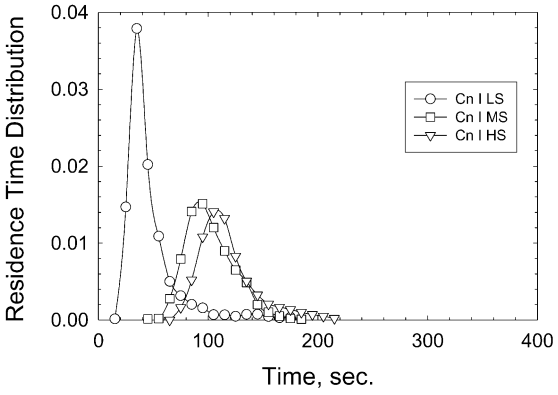

Fig. 6. Residence time distribution curves for the counter-rotating, non-intermeshing twin screw extruder outfitted with low (Cn NI LS), medium (Cn NI MS), and high (Cn NI HS) shear screw configurations.

The extruder type and screw configuration affects both the mean residence time and the residence time distribution in complex ways. The single screw extruder, with an intensive mixing head, has a relatively narrow residence time distribution or low degree of backmixing. Each of the twin screw extruders provide much more backmixing than the single screw extruder. The co-rotating intermeshing extruder gave the highest degree of backmixing while the counter-rotating intermeshing extruder gave the least. For these twin screw extruders, the screw configuration had only modest effects on the degree of backmixing. The counter-rotating non-intermeshing extruder gave intermediate degrees of backmixing that were more significantly affected by the screw configuration or shear intensity. For a given extruder type, the mean residence time generally increased while the degree of backmixing decreased, except for the co-rotating intermeshing extruder, as the screw was configured for more intense shearing (see Table 1). For the low shear screw configuration in the counter-rotating, intermeshing twin screw extruder, the mean residence time, 47 s, is quite short. Since the sampling time was for 10 s intervals, the residence time distribution curve was not defined accurately enough to calculate a meaningful variance.

Observation of the final shape of the aluminum pellets (~2 mm in diameter) spiked into the extruder to measure the residence time distribution also reveals important insight about the clearance, hence maximum shear rates in the various extruder configurations. When there are large clearances, the pellets exit the extruder with no change in size or shape. However, with some screw configurations the aluminum pellets were severely deformed since they could not pass through the metal-to-metal clearance without deformation. The counter-rotating, non-intermeshing extruder configurations yielded aluminum pellets that did

Table 1
Characterization of nanocomposites made via different extruders/screw configurations

Extruder and screw type	XRD basal spacing (Å)	XRD area under curve	TEM platelets or intercalates per 6.25 cm^2 (at 130,500 ×)	Extruder mean residence time (s)	Normalized variance σ^2
Single screw extruder					
30B	30.9	120	13	141	0.0049
15A	32.2	825	4	141	0.0049
Twin screw extruder					
Co-rotating intermeshing					
Low shear 15A	36.2	382	7	67	0.090
Medium shear 15A	37.7	146	16	153	0.113
Counter-rotating intermeshing					
Low shear 15A	34.4	263	8	47	
Medium shear 15A	38.0	106	14	102	0.0557
Medium shear 30B	No Peak	No Peak	35	102	0.0557
High shear 15A	37.9	164	10	117	0.049
Counter-rotating non-intermeshing					
Low shear 15A	34.7	581	11	108	0.0895
Medium shear 15A	No Peak	No Peak	27	162	0.0653
High shear 15A	37.9	277	20	136	0.0579

not deform in shape after passing through the extruder. Deformation of the pellets was observed in the intermeshing twin screw extruders.

The extruder screw configuration and process conditions, not explored during this study, of feedrate, temperature profile and screw rpm are critical to achieve delamination and distribution of the MMT platelets to make a high quality nanocomposite. The authors recognize there were limited numbers of experimental conditions explored in this study and that the screw configurations were not designed to allow a detailed understanding of the differentiation of the effects of shear intensity, mean residence time and residence time distribution. A more detailed study is required to understand screw configurations that will differentiate the effects of shear intensity, mean residence time and residence time distribution to achieve the desired exfoliation.

4. The effect of processing on nanocomposite morphology

The nanocomposites formed from 30B or 15A were selected for this work because of the differences in ease of delaminating and dispersing these two organoclays in polyamide 6. The organoclay designated 30B can easily be delaminated and dispersed in polyamide 6 while 15A, which has a different chemical treatment, does not delaminate and disperse easily in polyamide 6. Thus, 15A/polyamide 6 is a good model system for studying processing responses, because delamination and dispersion in this system is especially sensitive to the process conditions.

Representative XRD scans and TEM photomicrographs are shown in Figs. 8 and 9, respectively, while Table 1 summarizes results obtained from such observations over a broad range of process conditions. As seen in Fig. 8, the XRD peak position does not change a lot, but does increase with delamination as shown in the TEM photomicrographs in Fig. 9. The peak also decreases in height and gets broader as delamination increases. The changes seen in the XRD can be explained [8] by polymer entering the clay galleries pushing the platlets apart (i.e. intercalation). As more polymer enters the galleries, two possible changes can occur. First, the platelets can loose their ordered, crystalline structure and become disordered with the platelets no longer parallel without pushing the platelets apart. The result is that the XRD peak broadens into the baseline (intercalated disordered). Secondly, the polymer that enters the galleries pushes the platelets far enough apart that the platelet separation exceeds the sensitivity of XRD (exfoliation). TEM is the better tool to monitor dispersion because the clay platelets can be seen. The platelet count in a given area of the TEM photomicrographs, as described earlier, is used here to describe dispersion; high values indicate a more delaminated and dispersed nanocomposite.

The TEM results, expressed as the number of platelets or intercalates per unit area as given in Table 1, demonstrate that process conditions have a strong effect on the delamination and dispersion of the clay platelets. For each extruder and each screw configuration, 30B gave much better delamination than 15A. In the single screw extruder, 15A yields larger clay intercalates while 30B results in a partially delaminated nanocomposite. All of the twin screw extruders gave good delamination and dispersion with 30B, so only one sample made with 30B in a twin screw extruder has

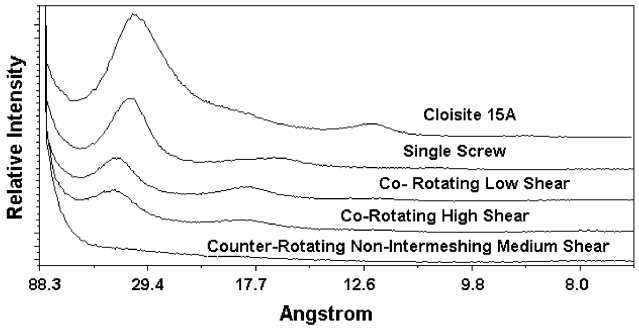

Fig. 8. Wide angle X-ray diffraction scans for selected nanocomposites prepared from 15A and polyamide 6 using different extruders and screw configurations. Peaks indicate the presence of incompletely dispersed platelets of organoclay.

been included for comparison. The shear intensity was changed in each of the three types of twin screw extruders to assess the effect of screw design on reducing the 8 μm particles to the individual delaminated platelets. For the co-rotating extruder, configurations producing low and medium shear intensity were employed. For the counter-rotating extruder, low, medium and high shear intensity screw configurations were used in both the intermeshing and non-intermeshing mode. For each of the twin screw extruder types, the best delamination and dispersion was obtained using the medium shear intensity screw configuration. Overall, the best dispersion and delamination of 15A was obtained using the counter-rotating, non-intermeshing medium shear extruder screw configuration. Thus, as the shear intensity was increased for a given extruder type from the medium to high shear intensity configuration, a degree of shear intensity was reached where delamination and dispersion did not increase, but got worse. It is interesting to note that for a given extruder type, the highest shear intensity configuration did not give the best delamination and dispersion. However, the most surprising result was that the non-intermeshing extruder gave the best delamination and dispersion. This extruder also allowed aluminum pellets to flow through the extruder without any deformation in shape. Thus, it appears that very high shear, dispersive mixing is not the key to delamination, at least for this system.

One might expect residence time in the extruder to be an important variable. Fig. 10 shows a plot of the TEM dispersion parameter for all the mixtures of 15A with polyamide 6 versus the mean residence time in each extruder type and screw configuration. While the data do not fall into a single unique relationship, there is a very clear trend of improved delamination as the residence time increases for all samples prepared in twin screw extruders. This trend might be anticipated based on the notion of diffusion of the polymer chains into the clay galleries [22]. Note, however, that delamination in the single screw extruder is poor in spite of the relatively long residence time. Since there is backmixing in the extruder, each fluid element does not spend the

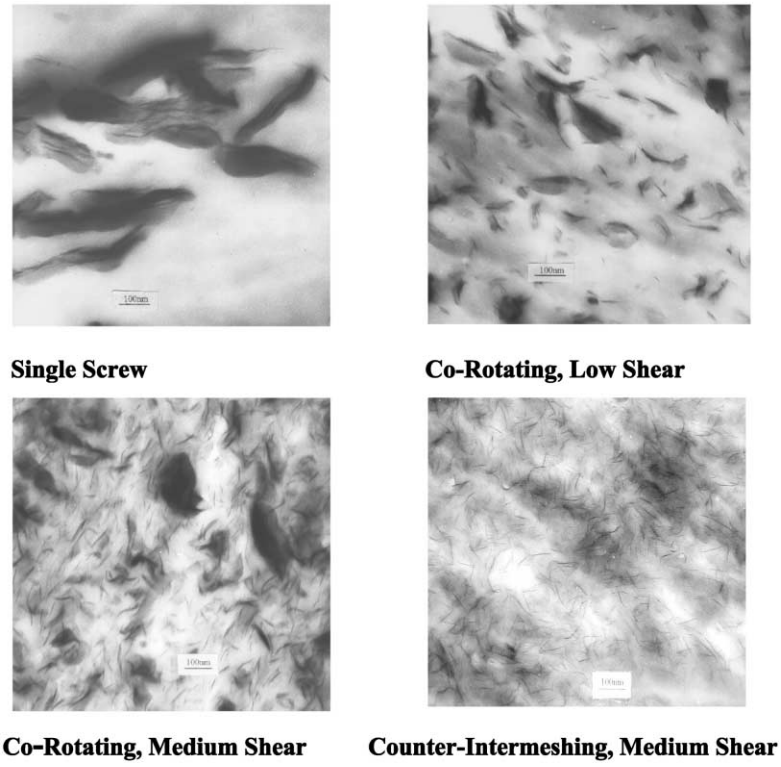

Fig. 9. Transmission electron photomicrographs for selected nanocomposites prepared from 15A and polyamide 6 using different extruders and screw configurations.

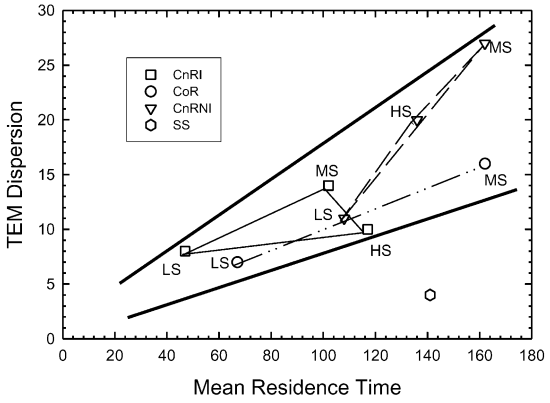

Fig. 10. TEM dispersion (see text for definition and method of measurement) of various nanocomposites of 15A and polyamide 6 plotted versus mean residence times (in seconds) computed as described in text.

same length of time in the extruder; thus, a simple relationship with mean residence time might not be expected. One might anticipate that the degree of delamination might also be a function of the degree of backmixing (or σ^2) since this is a measure of the distribution of residence times and, to some extent, reflects the extent of mixing in the extruder.

To test this idea, a multiple regression analysis of the following type was performed

$$(\mathrm{TEM}) = \sum_{i=0} \sum_{j=0} k_{ij} (\bar{t})^i (\sigma^2)^j \tag{6}$$

where (TEM) is the platelet count determined by transmission electron microscopy. Of course, the degree of correlation improves the more terms included in the model; however, due to the limited number of data in the available set, the number of fitting parameters must be kept small in order to be meaningful. Thus, the data for 15A/polyamide 6 was fitted to a model including up to quadratic terms in $\bar{t}$ and σ^2 but with no cross terms. The resulting model equation is given below

$$(\mathrm{TEM}) = -4.2 - 0.21\bar{t} + 564(\sigma^2) + 0.0017(\bar{t})^2 - 4100(\sigma^2)^2 \tag{7}$$

It fits the data with a correlation coefficient $R = 0.98$. Fig. 11a shows the experimental values of TEM dispersion, $(\mathrm{TEM})_{\mathrm{exp}}$, plotted versus the values calculated from Eq. (7), $(\mathrm{TEM})_{\mathrm{calc}}$. Fig. 11b shows a three dimensional plot of the experimental data and a representation of the surface given by Eq. (7). The fact that such a relation seems to exist is quite provocative. Over the range of variables shown, the degree of dispersion clearly increases with mean residence time: however, there seems to be an optimum level of backmixing which occurs at $\sigma^2 = 0.069$ (obtained by differentiation of Eq. (7)). For a given mean residence time, higher or lower values of (σ^2) appear to be detrimental to dispersion. It is premature to belabor the interpretation or mechanistic causes for such a relation, since it is based on such a small amount of data. Clearly, a more thorough validation of any such relation is needed.

5. Mechanical properties

The focus of this study was primarily to assess how extruder type and screw configuration affects delamination and dispersion; however, some limited mechanical property evaluations were made. The tensile modulus is shown as a function of TEM Dispersion in Fig. 12. The tensile modulus increases from 2.7 GPa for neat polyamide 6 to 3.3 GPa for a poorly dispersed and delaminated nanocomposite to 4.0 GPa for a well-dispersed and delaminated nanocomposite at 5 wt% of the 15A organoclay. Use of organoclay 30B, which is more compatible with polyamide 6, leads to a tensile modulus of 4.4 GPa. On the other hand, 30B leads to poorer elongation and impact results than 15A as shown in Table 2, even when the process conditions are changed to improve the delamination and dispersion of 15A. Because of the differences in organo-treatment and the loading level on the organoclays, the 15A and 30B mineral content is 3.1 and 3.7%, respectively. The higher mineral content of 30B partly explains the higher modulus and possibly explains the poorer elongation. Of course, exfoliation of clay into polyamide 6 influences properties other than modulus [23]; future papers will address these structure–property issues.

6. A proposed mechanism for delamination and dispersion

A mechanism for dispersion of organoclay into a polymer during melt processing, based mostly on the results of this work, is proposed. These ideas also draw on unpublished work by the authors on dispersing organoclay in homopolymer polypropylene and in a blend of polypropylene and maleated polypropylene. Similar attempts to disperse organoclay in polypropylene yield intercalants that are stacks of clay that by TEM look like the results from the single screw extruder shown in Fig. 9. The proposed mechanism, shown in Fig. 13a, based on the relationship between the compatibility of the chemistry of the clay treatment/resin matrix and the process conditions used to make a nanocomposite is described in three cases. The first case is chemistry dependent. When the clay chemical treatment and the resin are compatible, almost any set of processing conditions, except for the single screw extruder, but including a Brabender bowl mixer and a 2-roll mixer, can be used to form an exfoliated nanocomposite. A good example of Case 1 is polyamide 6 and 30B. In Case 2, clay chemical treatment and polymer are marginally compatible. In this situation, the process conditions can be optimized to give a good exfoliated nanocomposite. Polyamide 6 and 15A are an example of Case 2 behavior. The organoclay chemical treatment and the resin matrix are compatible enough that

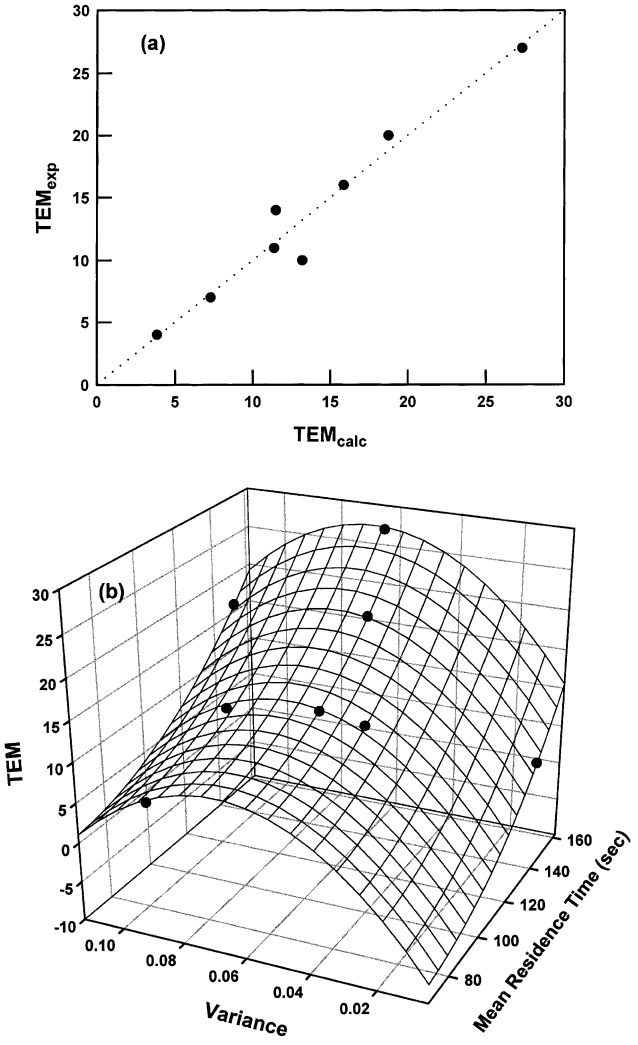

Fig. 11. Model representation (Eq. (7)) of TEM Dispersion for 15A/polyamide 6 nanocomposites. Part (a) shows comparison of experimental data (TEM_{exp}) with that calculated (TEM_{calc}) from Eq. (7). Part (b) shows three dimensional representation of TEM dispersion as a function of mean residence time ($\bar{t}$) and the variance (σ^2). Points are experimental data. Grid is surface defined by Eq. (7). Correlation coefficient for this model fit is $R = 0.98$.

extrusion conditions can be varied to optimize delamination and dispersion. Polypropylene and 15A represent Case 3, where there is no apparent compatibility of the clay chemical treatment and the polymer. Processing can be optimized to give intercalants or tactoids that are minimized in size, but even partial exfoliation does not occur. When one adds maleated polypropylene to the Case 3 example, compatibility between the polymer matrix and clay treatment increases, the system exhibits Case 2 behavior.

At the beginning of this study, the authors anticipated that increasing shear intensity would lead to improved exfoliation. The results of this work have shown this is not the complete solution to exfoliation. Fig. 13b shows possible clay delamination pathways. In Pathway 1, stacks of platelets are decreased in height by sliding platelets apart

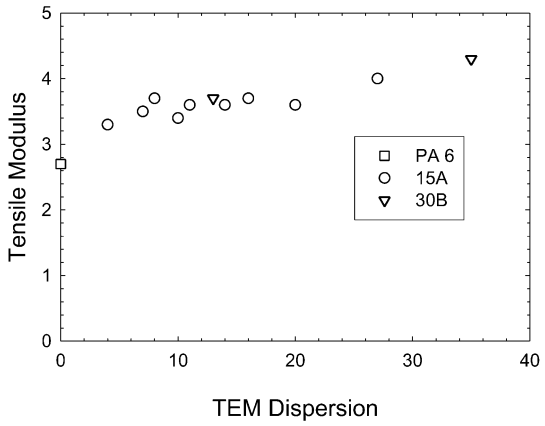

Fig. 12. Tensile modulus of nanocomposites containing (~3.1 to ~3.7% montmorillonite) as a function of the measured TEM dispersion.

from each other, a pathway that requires shear intensity. Pathway 2 shows polymer chains entering the clay galleries pushing the end of the platelets apart. This pathway does not require high shear intensity but involves diffusion of polymer into the clay galleries (driven by either physical or chemical affinity of the polymer for the organoclay surface) and is thus, facilitated by residence time in the

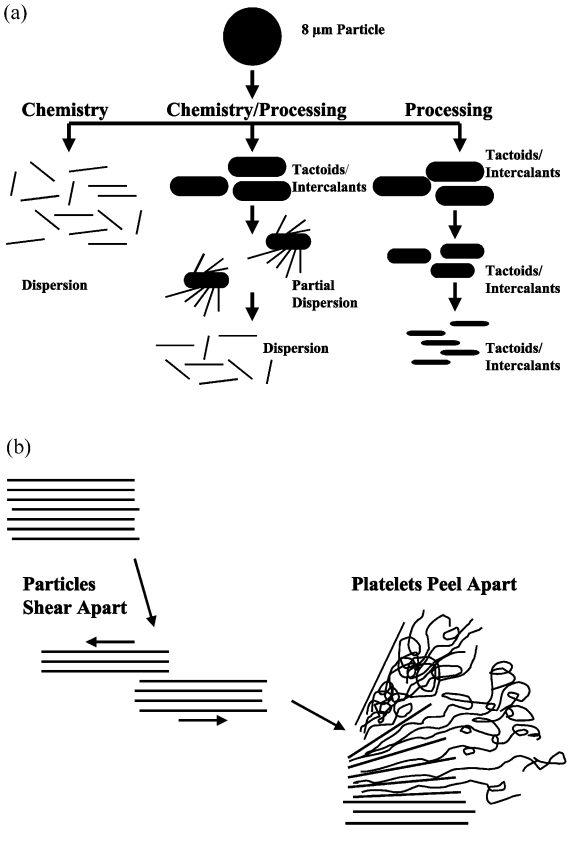

Fig. 13. Proposed mechanism of how the organoclay particles disperse into polymers during melt processing. Part (a) shows three cases involving the interplay between chemistry and process conditions in the extruder. Part (b) illustrates schematically how platelets peel apart under the action of shear.

Table 2
Mechanical properties of nanocomposites made via different extruders/screw configurations

Extruder and screw type	Tensile modulus (GPa)	Tensile yield strength (MPa)	% elongation 5.08 cm/min	% elongation 0.508 cm/min	Izod impact (J/m)
Capron B135WP	2.7	64	40	> 200	37
Single screw extruder					
30B	3.7	79	8	10	36
15A	3.3	77	26	37	50
Twin screw extruder					
Co-rotating intermeshing					
Low shear 15A	3.5	78	23	47	40
Medium shear 15A	3.7	81	35	143	40
Counter-rotating intermeshing					
Low shear 15A	3.7	77	45	168	45
Medium shear 15A	3.6	75	32	183	44
Medium shear 30B	4.4	89	10	12	37
High shear 15A	3.4	69	50	> 200	43
Counter-rotating non-intermeshing					
Low shear 15A	3.6	78	32	44	46
Medium shear 15A	4.0	85	17	39	44
High shear 15A	3.6	80	60	> 200	45

extruder. As more polymer enters and goes further in between clay platelets, especially near the edge of the clay galleries, the platelets appear to peel apart. It is important to note that the top platelet in the stack may be able to curl away as polymer enters from the edge since the platelets are able to bend. Two TEM photomicrographs representing this peeling mechanism obtained during this study are shown in Fig. 14. Thus, it appears that both pathways are involved. As clay is melt blended into a polymer, the clay particles are fractured by the shear in the extruder into tactoids or intercalants. Our experience for polypropylene with various organoclays, a Case 3 example, on a number of different extruders is that the particles are fractured to ribbon tactoids/intercalants about 100 nm thick. Unless something is done to increase chemical compatibility between the resin matrix and the clay treatment chemistry, adding more shear intensity to the extruder does not cause the particles to decrease further in size. Addition of compatibilizer, maleated polypropylene, and good process conditions will enable significant improvement in delamination and dispersion.

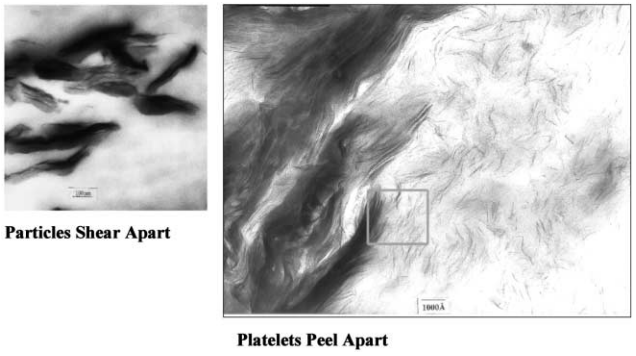

Fig. 14. TEM photomicrographic evidence for the process of peeling platelets apart during melt compounding.

7. Conclusions

It has been demonstrated that the degree of delamination and dispersion of layered silicate nanocomposites formed from polyamide 6 by melt compounding is affected by both the clay chemical treatment and the type of extruder and its screw design. Increasing the mean residence time in the extruder generally improves the delamination and dispersion. However, there appears to be an optimum extent of back mixing, as judged by the broadness of the residence time distribution and an optimum shear intensity; excessive shear intensity apparently causes poorer delamination and dispersion; excessive shear intensity or backmixing apparently cause poorer delamination and dispersion. A mechanism for delamination and dispersion is proposed which should be considered when designing a screw configuration. Shear intensity is required to start the dispersion process, by shearing particles apart into tactoids or intercalants. Residence time in a low shearing or mildly shearing environment is required to allow polymer to enter the clay galleries and peel the platelets apart.

The non-intermeshing twin screw extruder used in this study yielded the best delamination and dispersion. It is believed that excellent delamination and dispersion can be achieved with both co-rotating and counter-rotating, intermeshing types of extruders when a fully optimized screw configuration is used. It is recognized that the extruder process conditions are important variables that

must be optimized to effect a high degree of delamination and dispersion.

Acknowledgements

The authors would like to thank Randy Chapman of Southern Clay Products for XRD scans, Peggy Miller of The University of Texas Health Science Center in San Antonio for the TEM photomicrographs. Work at The University of Texas at Austin was supported by the Texas Advanced Technology Program under Grant Numbers 003658-0017 and -0067.

References

[1] Carter LW, Hendricks JG, Bolley DS. United States Patent No. 2,531,396, 1950 (assigned to National Lead Co).
[2] Fujiwara S, Sakamoto T. Japanese Patent Application No. 109,998, 1976 (assigned to Unitika K.K.).
[3] Usuki A, Kojima Y, Kawasumi M, Okada A, Fukushima Y, Kurauchi T, Kamigatio O. J Mater Res 1993;8:1179.
[4] Usuki A, Koiwai A, Kojima Y, Kawasumi M, Okada A, Kurauchi T, Kamigaito O. J Appl Polym Sci 1995;55:119.
[5] Okada A, Usuki A. Mater Sci Engng C 1995;3:109.
[6] Okada A, Fukushima Y, Kawasumi M, Inagaki S, Usuki A, Sugiyama S, Kurauchi T, Kamigaito O. United States Patent No. 4,739,007, 1988 (assigned to Toyota Motor Co., Japan).
[7] Dennis HR, Hunter DL, Chang D, Kim S, White JL, Cho JW, Paul DR. SPE ANTEC Tech Pap 2000;40:428.
[8] Gilman JW, Morgan AB, Giannelis EP, Wuthenow M, Manias E. Proceedings of the BCC Conference on Flame Retardancy. 1999. p. 10.
[9] Nahin PG, Backlund PS. United States Patent No. 3,084,117, 1963 (assigned to Union Oil Co).
[10] Vaia RA, Hope I, Giannelis EP. Chem Mater 1993;5:1694.
[11] Vaia RA, Jandt KD, Kramer EJ, Giannelis EP. Chem Mater 1996;8:2628.
[12] Vaia RA, Giannelis EP. Macromolecules 1997;30:7990.
[13] Vaia RA, Giannelis EP. Macromolecules 1997;30:8000.
[14] Christiani BR, Maxfield M. United States Patent No. 5,747,560, 1998 (assigned to AlliedSignal).
[15] Liu L, Qi Z, Zhu XJ. Appl Polym Sci 1999;71:1133.
[16] Vaia RA, Tse OK, Giannelis EP. United States Patent No. 5,955,535, 1999 (assigned to Cornell Research Foundation, Inc).
[17] Lan T, Kaviratna PD, Pinnavaia T. J Chem Mater 1995;7:2144.
[18] Lan T, Pinnavaia TJ. Mater Res Soc Symp Proc 1966;435:79.
[19] Shon K, Chang D, White JL. Int Polym Process 1999;8:44.
[20] Lim S, White JL. Int Polym Process 1994;9:33.
[21] Bang DS, Hong MH, White JL. Polym Engng Sci 1998;38:485.
[22] Vaia RA, Jandt KD, Kramer EJ, Giannelis EP. Macromolecules 1995;28:8080.
[23] Shelley JS, Mather PT, DeVries KL. Polymer 2001;42:5849.